ICASSP 2024 - 2024 IEEE International Conference on Acoustics, Speech and Signal Processing (ICASSP) | 979-8-3503-4485-1/24/$31.00 ©2024 IEEE | DOI: 10.1109/ICASSP48485.2024.10446959

GRIDLESS PARAMETER ESTIMATION IN PARTLY CALIBRATED RECTANGULAR ARRAYS

Tianyi Liu[1], *Sai Pavan Deram*[2], *Khaled Ardah*[3], *Martin Haardt*[4], *Marc E. Pfetsch*[5], *Marius Pesavento*[1]

[1]Communication Systems Group, Technical University of Darmstadt, Germany
[2]IMDEA Networks, Spain
[3]Lenovo Research 5G Lab, Lenovo, Germany
[4]Communications Research Laboratory, Ilmenau University of Technology, Germany
[5]Research Group Optimization, Technical University of Darmstadt, Germany

ABSTRACT

Spatial frequency estimation from a mixture of noisy sinusoids finds applications in various fields. The widely used subspace-based methods provide super-resolution parameter estimation at a low computational cost. However, they require an accurate array calibration, which is difficult for large antenna arrays. Sparsity-based methods have been shown to be more robust than subspace-based methods in difficult scenarios, e.g., in the case with a small number of snapshots and/or correlated sources. In this paper, we consider the direction-of-arrival (DOA) estimation in partly calibrated rectangular arrays comprising several calibrated and identical subarrays. We derive a gridless sparse formulation for DOA estimation based on the shift-invariance properties of the array and develop an efficient algorithm in the alternating direction method of multipliers (ADMM) framework. Numerical simulations show the superior error performance of our proposed method compared to subspace-based methods.

Index Terms— DOA estimation, joint sparsity, partly calibrated arrays, shift-invariance, ADMM

1. INTRODUCTION

Direction-of-arrival (DOA) estimation methods like MUSIC [1] and ESPRIT [2, 3] are known to be sensitive to fluctuations and uncertainties in the array geometry [4] and require an accurate array calibration [5]. With the increasing array size, array calibration becomes more difficult. As a solution, the concept of partly calibrated arrays (PCAs) has been introduced by partitioning the entire array into fully calibrated subarrays with uncertain phase relation between subarrays [6, 7].

Recently, several DOA estimation methods for PCAs have been introduced [2, 7–9]. Search-free subspace-based methods are proposed in [2, 7, 8] for PCAs with identical subarrays. Differently, the authors in [9] propose a search-based method, which applies to arbitrary subarray topologies. However, the search-based methods require an expensive spectral search. Subspace-based methods suffer from performance degradation in difficult scenarios, e.g., in the cases with highly correlated source signals and/or a small number of measurements. To overcome those issues, sparsity-based methods have been considered [10, 11]. The authors in [10] propose a grid-based sparse DOA estimation method for PCAs, which, however, may suffer from basis mismatch due to the spectrum discretization. A gridless sparse method that avoids the sampling over the field-of-view (FOV), termed shift-invariant SPARROW (SI-SPARROW), is devised in [12] for PCAs. Although the above sparse methods show a good error performance even in difficult scenarios, both of them assume a uniform linear subarray structure, which allows DOA estimation only in the azimuth direction.

In this paper, we extend the SI-SPARROW formulation in [12] to the case with a partly calibrated rectangular array (PCRA) with identical subarrays and unknown intersubarray displacements, which allows DOA estimation in both azimuth and elevation directions. In contrast to the SDP reformulation approach in [12], we develop an efficient algorithm under the ADMM framework for the established SI-SPARROW problem. Numerical simulations show that our proposed method outperforms the subspace-based methods in challenging scenarios. Moreover, compared to the SDP implementation in [12], the ADMM-based solution approach for the SI-SPARROW problem exhibits a significantly reduced computational cost in the oversampled case.

2. SIGNAL MODEL

Consider an $M_x \times M_y$ partly calibrated rectangular array (PCRA), as shown in Fig. 1(a), composed of $P_x \times P_y$ identical subarrays of $L_x \times L_y$ sensors with $M_x = P_x L_x$ and $M_y = P_y L_y$. Let $M = M_x M_y$ be the total number of sensors in the PCRA. Let Δ_p^x (resp., Δ_p^y) be the *unknown* intersubarray displacement between the first and the pth subarray along the

This work was supported in part by the DFG PRIDE Project PE 2080/2-1 and in part by the EXPRESS II Project within the DFG priority program CoSIP (DFG-SPP 1798).

x-axis (resp., y-axis), while the *perfectly known* relative position of the lth sensor along the x-axis (resp., y-axis) within each subarray is denoted by δ_l^x (resp., δ_l^y). Moreover, we assume that N_S narrowband far-field source signals impinge from distinct unknown DOAs with different azimuth and elevation angles, denoted by $\phi_i \in [-180°, 180°)$ and $\theta_i \in [0°, 90°]$, respectively, $i=1,...,N_S$. Each direction (ϕ_i, θ_i) can be equivalently represented by a pair of spatial frequencies in the two dimensions defined as $\mu_i^x = \pi \cos(\phi_i)\sin(\theta_i) \in [-\pi, \pi)$ and $\mu_i^y = \pi \sin(\phi_i)\sin(\theta_i) \in [-\pi, \pi)$, respectively. The spatial frequencies of the N_S sources are collected in $\boldsymbol{\mu} = [\boldsymbol{\mu}^{x\mathsf{T}}, \boldsymbol{\mu}^{y\mathsf{T}}]^\mathsf{T}$ with $\boldsymbol{\mu}^x = [\mu_1^x, ..., \mu_{N_S}^x]^\mathsf{T}$ and $\boldsymbol{\mu}^y = [\mu_1^y, ..., \mu_{N_S}^y]^\mathsf{T}$. Let $\boldsymbol{Y} \in \mathbb{C}^{M \times N}$ be the measurement matrix that contains the array output in N time-slots, which is modeled as

$$\boldsymbol{Y} = \boldsymbol{A}(\boldsymbol{\mu})\boldsymbol{\Psi} + \boldsymbol{N}. \tag{1}$$

The matrix $\boldsymbol{\Psi} \in \mathbb{C}^{N_S \times N}$ contains the source waveforms with $\psi_{i,n}$ being the waveform from source i at time instant n. The matrix $\boldsymbol{N} \in \mathbb{C}^{M \times N}$ contains the independent and identically distributed noise entries of distribution $\mathcal{CN}(0, \sigma_n^2)$. The matrix $\boldsymbol{A}(\boldsymbol{\mu}^x, \boldsymbol{\mu}^y) \in \mathbb{C}^{M \times N_S}$ collects the N_S steering vectors as

$$\boldsymbol{A}(\boldsymbol{\mu}) = \big[\boldsymbol{a}(\mu_1^x, \mu_1^y) \quad ... \quad \boldsymbol{a}(\mu_{N_S}^x, \mu_{N_S}^y)\big], \tag{2}$$

where $\boldsymbol{a}(\mu_i^x, \mu_i^y) \in \mathbb{C}^M$ is the array dependent steering vector corresponding to source i. For the considered PCRA, the array steering vector in the direction (μ^x, μ^y) is expressed as the Kronecker product $\boldsymbol{a}(\mu^x, \mu^y) = \boldsymbol{a}_x(\mu^x) \otimes \boldsymbol{a}_y(\mu^y)$ with

$$\boldsymbol{a}_x(\mu^x) = [1, ..., \mathrm{e}^{\mathrm{j}\mu^x \delta_{L_x}^x}, \mathrm{e}^{\mathrm{j}\mu^x \Delta_2^x}, ..., \mathrm{e}^{\mathrm{j}\mu^x (\Delta_{P_x}^x + \delta_{L_x}^x)}]^\mathsf{T},$$
$$\boldsymbol{a}_y(\mu^y) = [1, ..., \mathrm{e}^{\mathrm{j}\mu^y \delta_{L_y}^y}, \mathrm{e}^{\mathrm{j}\mu^y \Delta_2^y}, ..., \mathrm{e}^{\mathrm{j}\mu^y (\Delta_{P_y}^y + \delta_{L_y}^y)}]^\mathsf{T}.$$

In the following we introduce the shift-invariance properties of the array. To this end, we define the selection matrices

$$\boldsymbol{J}_p^x = \boldsymbol{e}_{P_x,p} \otimes \boldsymbol{I}_{L_x} \otimes \boldsymbol{I}_{P_y} \otimes \boldsymbol{I}_{L_y}, \qquad p=1,...,P_x, \tag{3a}$$
$$\boldsymbol{K}_l^x = \boldsymbol{I}_{P_x} \otimes \boldsymbol{e}_{L_x,l} \otimes \boldsymbol{I}_{P_y} \otimes \boldsymbol{I}_{L_y}, \qquad l=1,...,L_x, \tag{3b}$$
$$\boldsymbol{J}_p^y = \boldsymbol{I}_{P_x} \otimes \boldsymbol{I}_{L_x} \otimes \boldsymbol{e}_{P_y,p} \otimes \boldsymbol{I}_{L_y}, \qquad p=1,...,P_y, \tag{3c}$$
$$\boldsymbol{K}_l^y = \boldsymbol{I}_{P_x} \otimes \boldsymbol{I}_{L_x} \otimes \boldsymbol{I}_{P_y} \otimes \boldsymbol{e}_{L_y,l}, \qquad l=1,...,L_y, \tag{3d}$$

to assign sensors to various shift-invariant groups, where $\boldsymbol{e}_{P,p} = [0,...,0,1,0,...,0]^\mathsf{T}$ is the P-dimensional basis vector with the pth entry being one and all the other entries being zero. As depicted in Fig. 1, by the operation $\boldsymbol{J}_p^{x\mathsf{T}}\boldsymbol{a}$ (resp., $\boldsymbol{J}_p^{y\mathsf{T}}\boldsymbol{a}$), the responses of all subarrays at the pth position in the x-axis (resp., y-axis) are selected. Similarly, $\boldsymbol{K}_l^x$ and $\boldsymbol{K}_l^y$ are used to select all sensors at the lth position in the x-axis and y-axis, respectively, within the subarrays. Then the shift-invariance properties of the steering matrix are expressed as

$$\boldsymbol{J}_p^{x\mathsf{T}}\boldsymbol{A}(\boldsymbol{\mu}) = \boldsymbol{J}_1^{x\mathsf{T}}\boldsymbol{A}(\boldsymbol{\mu})\boldsymbol{\Phi}^{\Delta_p^x}(\boldsymbol{\mu}^x), \qquad p=2,...,P_x, \tag{4a}$$
$$\boldsymbol{K}_l^{x\mathsf{T}}\boldsymbol{A}(\boldsymbol{\mu}) = \boldsymbol{K}_1^{x\mathsf{T}}\boldsymbol{A}(\boldsymbol{\mu})\boldsymbol{\Phi}^{\delta_l^x}(\boldsymbol{\mu}^x), \qquad l=2,...,L_x, \tag{4b}$$
$$\boldsymbol{J}_p^{y\mathsf{T}}\boldsymbol{A}(\boldsymbol{\mu}) = \boldsymbol{J}_1^{y\mathsf{T}}\boldsymbol{A}(\boldsymbol{\mu})\boldsymbol{\Phi}^{\Delta_p^y}(\boldsymbol{\mu}^y), \qquad p=2,...,P_y, \tag{4c}$$
$$\boldsymbol{K}_l^{y\mathsf{T}}\boldsymbol{A}(\boldsymbol{\mu}) = \boldsymbol{K}_1^{y\mathsf{T}}\boldsymbol{A}(\boldsymbol{\mu})\boldsymbol{\Phi}^{\delta_l^y}(\boldsymbol{\mu}^y), \qquad l=2,...,L_y, \tag{4d}$$

where $\boldsymbol{\Phi}(\boldsymbol{\mu}^x) = \mathrm{Diag}(\mathrm{e}^{\mathrm{j}\mu_1^x}, ..., \mathrm{e}^{\mathrm{j}\mu_{N_S}^x}) \in \mathbb{C}^{N_S \times N_S}$ and $\boldsymbol{\Phi}(\boldsymbol{\mu}^y) = \mathrm{Diag}(\mathrm{e}^{\mathrm{j}\mu_1^y}, ..., \mathrm{e}^{\mathrm{j}\mu_{N_S}^y}) \in \mathbb{C}^{N_S \times N_S}$ contain the phase shifts for

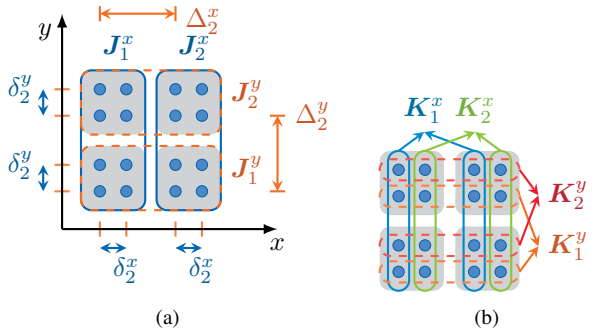

Fig. 1. Different shift-invariant groups for a PCRA composed of 2×2 subarrays with 2×2 sensors per subarray.

frequencies $\boldsymbol{\mu}^x$ and $\boldsymbol{\mu}^y$ on their main diagonal, respectively. Also, due to the narrowband assumption, the responses of each pair of sensors differ only in a phase shift. This shift-invariance property is similarly expressed as

$$\boldsymbol{e}_{M,m}^\mathsf{T}\boldsymbol{A}(\boldsymbol{\mu}) = \boldsymbol{e}_{M,1}^\mathsf{T}\boldsymbol{A}(\boldsymbol{\mu})\boldsymbol{\Phi}^{(\Delta_p^x + \delta_k^x)}(\boldsymbol{\mu}^x)\boldsymbol{\Phi}^{(\Delta_q^y + \delta_l^y)}(\boldsymbol{\mu}^y) \tag{5}$$

for $p=1,...,P_x$, $q=1,...,P_y$, $k=1,...,L_x$, $l=1,...,L_y$ and $m = ((p-1)L_x + (k-1))M_y + (q-1)L_y + l$. More shift-invariances can be exploited if other array topologies are given, e.g., shift-invariances with overlapping groups. For simplicity, we limit our discussion to the example of the PRCA in Fig. 1.

Since the sensor displacements δ_l^x and δ_l^y are known, the shift-invariance equations in (4b) and (4d) can be used to estimate the spatial frequencies $\boldsymbol{\mu}$ by the 2D-ESPRIT methods in [13–15], with automatic pairing.

3. SPARSE SIGNAL FORMULATION

We define a sparse representation corresponding to (1) as

$$\boldsymbol{Y} = \boldsymbol{A}(\boldsymbol{\nu})\boldsymbol{X} + \boldsymbol{N}, \tag{6}$$

where $\boldsymbol{A}(\boldsymbol{\nu}) \in \mathbb{C}^{M \times K}$ is an overcomplete dictionary constructed according to (2) by sampling the FOV in $K \gg N_S$ directions with frequencies $\boldsymbol{\nu} = [\boldsymbol{\nu}^{x\mathsf{T}}, \boldsymbol{\nu}^{y\mathsf{T}}]^\mathsf{T}$, where $\boldsymbol{\nu}^x = [\nu_1^x, ..., \nu_K^x]^\mathsf{T}$ and $\boldsymbol{\nu}^y = [\nu_1^y, ..., \nu_K^y]^\mathsf{T}$, and $\boldsymbol{X} \in \mathbb{C}^{K \times N}$ is the sparse representation of the waveform matrix $\boldsymbol{\Psi}$. Provided that the true frequencies $\boldsymbol{\mu}$ are contained in the frequency grid, i.e., $\{(\mu_i^x, \mu_i^y)\}_{i=1}^{N_S} \subset \{(\nu_k^x, \nu_k^y)\}_{k=1}^K$, then $\boldsymbol{X} = [\boldsymbol{x}_1, ..., \boldsymbol{x}_K]^\mathsf{T}$ admits a row-sparse structure, which has only N_S nonzero rows corresponding to the N_S sources. For simplicity, in the rest of the paper, the dictionary is referred to as $\boldsymbol{A} = \boldsymbol{A}(\boldsymbol{\nu})$. With the model in (6), the DOA estimation is formulated as the well-known convex mixed-norm minimization

$$\min_{\boldsymbol{X} \in \mathbb{C}^{K \times N}} \quad \tfrac{1}{2}\|\boldsymbol{Y} - \boldsymbol{A}\boldsymbol{X}\|_\mathsf{F}^2 + \lambda\sqrt{N}\|\boldsymbol{X}\|_{2,1}, \tag{7}$$

where $\lambda > 0$ is the regularization parameter and the $\ell_{2,1}$-norm is defined as $\|\boldsymbol{X}\|_{2,1} = \sum_{k=1}^K \|\boldsymbol{x}_k\|_2$. In [11], the mixed-norm minimization problem (7) is equivalently reformulated as the SPARse ROW-norm reconstruction (SPARROW) problem

$$\min_{\boldsymbol{S} \in \mathbb{D}_+^K} \quad \mathrm{tr}\big((\boldsymbol{A}\boldsymbol{S}\boldsymbol{A}^\mathsf{H} + \lambda\boldsymbol{I}_M)^{-1}\widehat{\boldsymbol{R}}\big) + \mathrm{tr}(\boldsymbol{S}), \tag{8}$$

where $\widehat{\boldsymbol{R}} = \boldsymbol{Y}\boldsymbol{Y}^\mathsf{H}/N$ is the sample covariance matrix and $\mathbb{D}_+^K$ the set of $K \times K$ nonnegative diagonal matrices. The mini-

mizers $\widehat{\boldsymbol{X}}$ and $\widehat{\boldsymbol{S}}$ of problems (7) and (8), respectively, are related by $\hat{s}_{k,k}=\|\hat{\boldsymbol{x}}_k\|_2$ for $k=1,...,K$. Problem (8) can be further reformulated as a semidefinite program (SDP), which can be solved by an interior-point solver, e.g., MOSEK [16]. Alternatively, a customized algorithm for problem (8) based on coordinate descent is devised in [11], which is more scalable than the SDP implementation for large array size.

The grid-based formulation (8) suffers two drawbacks. First, the on-grid assumption is usually not satisfied due to the limited grid size, which results in spectral leakage effects and basis mismatch [17, 18] in the recovered signal. Second, the construction of the dictionary $\boldsymbol{A}$ requires the complete array calibration. Thus, we develop in the following a gridless approach by relaxing the grid-based SPARROW problem (8).

A straightforward gridless extension of problem (8) consists in jointly learning a dictionary $\boldsymbol{A}$ in the array manifold. With a slack variable $\boldsymbol{Q}$, this gridless extension is written as

$$\min_{\boldsymbol{S}\in\mathbb{D}_+^K,\boldsymbol{A}\in\mathcal{A}^K,\boldsymbol{Q}\in\mathbb{S}_+^M} \quad M\mathrm{tr}\big((\boldsymbol{Q}+\lambda\boldsymbol{I}_M)^{-1}\widehat{\boldsymbol{R}}\big)+\mathrm{tr}(\boldsymbol{Q}) \tag{9a}$$

$$\text{s.t.} \quad \boldsymbol{Q}=\boldsymbol{A}\boldsymbol{S}\boldsymbol{A}^{\mathsf{H}}, \tag{9b}$$

where $\mathcal{A}^K=\{\boldsymbol{A}(\boldsymbol{\nu})|\boldsymbol{\nu}\in[-\pi,\pi]^{2K},\ (\nu_i^x,\nu_i^y)\neq(\nu_j^x,\nu_j^y)\ \forall i,j=1,...,K,\ i\neq j\}$ is the array manifold with K distinct frequencies, and $\mathbb{S}_+^M$ denotes the set of $M\times M$ positive semidefinte Hermitian matrices. The equivalence between the objective functions in (9a) and (8) comes from the fact that $\mathrm{tr}(\boldsymbol{A}\boldsymbol{S}\boldsymbol{A}^{\mathsf{H}})=M\mathrm{tr}(\boldsymbol{S})$ as the steering vectors contain unit-modulus entries. The objective function in the reformulation (9) depends only on $\boldsymbol{Q}$ whose structure is specified by the dictionary-based constraint (9b). Also, the trace-term $\mathrm{tr}(\boldsymbol{Q})$ in (9a) encourages the rank-sparsity of $\boldsymbol{Q}$ as it is equivalent to the nuclear norm of $\boldsymbol{Q}$ for $\boldsymbol{Q}\succeq 0$ [19]. From the reformulation (9), one may obtain a simple gridless relaxation by discarding the dictionary-specific structural constraint (9b). This is equivalent to relaxing the array manifold $\mathcal{A}^K$ to be the complete space $\mathbb{C}^{M\times K}$ and, naturally, results in a poor accuracy on the estimated DOAs. Hence, we introduce several structural constraints on $\boldsymbol{Q}$ in place of the dictionary-based constraint (9b). Applying the shift-invariance properties in (4) to the dictionary $\boldsymbol{A}(\boldsymbol{\nu})$, we obtain the following set of structural constraints that are necessary for the constraint (9b):

$$\boldsymbol{J}_p^{x\mathsf{T}}\boldsymbol{Q}\boldsymbol{J}_p^x=\boldsymbol{J}_1^{x\mathsf{T}}\boldsymbol{Q}\boldsymbol{J}_1^x, \qquad p=2,...,P_x, \tag{10a}$$

$$\boldsymbol{K}_l^{x\mathsf{T}}\boldsymbol{Q}\boldsymbol{K}_l^x=\boldsymbol{K}_1^{x\mathsf{T}}\boldsymbol{Q}\boldsymbol{K}_1^x, \qquad l=2,...,L_x, \tag{10b}$$

$$\boldsymbol{J}_p^{y\mathsf{T}}\boldsymbol{Q}\boldsymbol{J}_p^y=\boldsymbol{J}_1^{y\mathsf{T}}\boldsymbol{Q}\boldsymbol{J}_1^y, \qquad p=2,...,P_y, \tag{10c}$$

$$\boldsymbol{K}_l^{y\mathsf{T}}\boldsymbol{Q}\boldsymbol{K}_l^y=\boldsymbol{K}_1^{y\mathsf{T}}\boldsymbol{Q}\boldsymbol{K}_1^y, \qquad l=2,...,L_y, \tag{10d}$$

$$q_{ii}=q_{11}, \qquad i=2,...,M. \tag{10e}$$

The structural constraints (10) essentially require that, for any pair of shift-invariant sensor groups, the corresponding submatrices in $\boldsymbol{Q}$ must be identical. Thus, the constraints (10) define a subspace of $M\times M$ Hermitian matrices, which is denoted by $\mathcal{T}^M$. Let $f(\boldsymbol{Q})$ denote the function in (9a). Replacing the dictionary-based constraint (9b) by the structural constraints (10), we obtain the following gridless shift-invariant SPARROW (SI-SPARROW) problem:

$$\min_{\boldsymbol{Q}\in\mathbb{S}_+^M\cap\mathcal{T}^M} \quad f(\boldsymbol{Q}). \tag{11}$$

Since, in the original problem (9), $\boldsymbol{Q}$ is designed to span the same subspace as the steering matrix $\boldsymbol{A}$, the solution $\widehat{\boldsymbol{Q}}$ of problem (11) can be used in place of the sample covariance matrix $\widehat{\boldsymbol{R}}$ in the 2D-ESPRIT discussed in Section 2 to estimate the spatial frequencies in a search-free manner.

Similar to the grid-based formulation, problem (11) can be reformulated as a SDP problem and solved by a state-of-the-art interior-point solver. However, to further reduce the computational cost, we develop in the next section an algorithm for problem (11) under the ADMM framework.

4. ADMM ALGORITHM FOR SI-SPARROW

In this section, we solve the SI-SPARROW problem (11) using the ADMM algorithmic framework. The choice of ADMM is motivated by the fact that problem (11) can be easily solved when only one of the two kinds of constraints, i.e., either the PSD constraint or the shift-invariance constraints, needs to be fulfilled. Specifically, the ADMM framework is employed to decompose the problem such that, in each subproblem, only one of the constraints needs to be fulfilled.

To apply the ADMM framework, we first write problem (11) as the following equivalent formulation:

$$\min_{\boldsymbol{Q}\in\mathcal{T}^M,\boldsymbol{Z}\in\mathbb{S}^M} \quad f(\boldsymbol{Q})+g(\boldsymbol{Z}) \tag{12a}$$

$$\text{s.t.} \quad \boldsymbol{Q}-\boldsymbol{Z}=\boldsymbol{0}, \quad \boldsymbol{Q}+\lambda\boldsymbol{I}_M\succ 0, \tag{12b}$$

where g is the indicator function of the PSD cone $\mathbb{S}_+^M$. In the reformulation (12), by introducing an auxiliary variable $\boldsymbol{Z}$, the shift-invariance constraints (10) are separated from the PSD constraint $\boldsymbol{Q}\succeq 0$ so that the two types of constraints can be addressed alternatingly. The positive definiteness constraint in (12b) is redundant as it is a necessary condition of $\boldsymbol{Q}=\boldsymbol{Z}\succeq 0$. However, it is required to ensure the convexity of the primal subproblem in ADMM that is introduced in (14a), since f is convex only in the subset where $\boldsymbol{Q}+\lambda\boldsymbol{I}_M\succ 0$.

The augmented Lagrangian of problem (12) is [20]

$$L_\rho(\boldsymbol{Q},\boldsymbol{Z},\boldsymbol{U})=f(\boldsymbol{Q})+g(\boldsymbol{Z})+\tfrac{\rho}{2}\|\boldsymbol{Q}-\boldsymbol{Z}+\boldsymbol{U}\|_{\mathsf{F}}^2, \tag{13}$$

where $\rho>0$ is the penalty parameter and $\boldsymbol{U}\in\mathbb{S}^M$ is the scaled dual variable. Let $\boldsymbol{Q}^{(t)},\boldsymbol{Z}^{(t)},\boldsymbol{U}^{(t)}$ be the value of the primal and dual variables at iteration t. The scaled form of ADMM for problem (12) consists of the three steps in each iteration:

$$\boldsymbol{Q}^{(t+1)}=\mathrm{argmin}_{\boldsymbol{Q}\in\mathcal{T}^M}\ f(\boldsymbol{Q})+\tfrac{\rho}{2}\|\boldsymbol{Q}-\boldsymbol{Z}^{(t)}+\boldsymbol{U}^{(t)}\|_{\mathsf{F}}^2$$

$$\text{s.t.} \quad \boldsymbol{Q}+\lambda\boldsymbol{I}_M\succ 0, \tag{14a}$$

$$\boldsymbol{Z}^{(t+1)}=\mathcal{P}_{\mathbb{S}_+^M}\big(\boldsymbol{Q}^{(t+1)}+\boldsymbol{U}^{(t)}\big), \tag{14b}$$

$$\boldsymbol{U}^{(t+1)}=\boldsymbol{U}^{(t)}+\boldsymbol{Q}^{(t+1)}-\boldsymbol{Z}^{(t+1)}. \tag{14c}$$

The operation $\mathcal{P}_{\mathbb{S}_+^M}$ is the projection onto the PSD cone $\mathbb{S}_+^M$, which can be obtained by truncating the eigenvalue decomposition (EVD) of the argument [21]. In the $\boldsymbol{Q}$-update (14a), a

proximal mapping from $\boldsymbol{Z}^{(t)}-\boldsymbol{U}^{(t)}$ is performed, which has no closed-form solution. However, as subproblem (14a) is convex, it can be easily solved by, e.g., the successive convex approximation (SCA) framework [22] with a proper approximate function. The convergence of the ADMM algorithm applied to the considered convex problem (12) can be easily verified according to the conditions given in [20, Sec. 3.2].

5. SIMULATION RESULTS

We conduct numerical experiments on synthetic data to evaluate the performance of the developed SI-SPARROW method for a PCRA. The complexity of the ADMM-based algorithm developed in Section 4 is compared to that of the SDP approach in [12]. The SDP reformulation is modeled by CVX [23, 24] and solved by the interior-point solver MOSEK [16]. From the estimated matrix $\widehat{\boldsymbol{Q}}$, the frequencies can be recovered by the multidimensional ESPRIT (MD-ESPRIT) method that is implemented by the simultaneous diagonalization or Schur decomposition [13, 25], given the shift-invariance equations in (4b) and (4d) with the known sensor displacements δ_l^x and δ_l^y. However, MD-ESPRIT can only consider a single shift-invariance equation in each dimension. To utilize all the shift-invariance equations in (4b) and (4d), we extend MD-ESPRIT by the following two steps. First, MD-ESPRIT is applied to the multiple shift-invariance equations by treating each shift-invariance equation as a virtual dimension. It recovers the diagonal matrices $\boldsymbol{\Phi}^{\delta_l^x}(\boldsymbol{\mu}^x)$ and $\boldsymbol{\Phi}^{\delta_l^y}(\boldsymbol{\mu}^y)$ in (4), whose entries form the 1D subarray steering vectors corresponding to each frequency to be estimated, i.e., μ_i^x and μ_i^y, respectively. Then the recovery of the frequencies can be performed independently from each estimated 1D steering vector by a single-source recovery method, e.g., root-MUSIC [26] in the special case where the sensors in each subarray are placed uniformly in each dimension. The method described above is referred to as multi-invariance multidimensional ESPRIT (MI-MD-ESPRIT).

We consider $N_S{=}2$ sources with $\boldsymbol{\mu}^x{=}[0.5{,}0.8]^\mathsf{T}$ and $\boldsymbol{\mu}^y{=}[1.5{,}1.2]^\mathsf{T}$ that follow a zero-mean complex normal distribution with unit variance and the correlation coefficient $\varphi{=}0.99$. The simulation scenario includes a PCRA with $2{\times}2$ subarrays. Each subarray is a uniform rectangular array with half-wavelength sensor spacing and each subarray contains $L_x{=}4$ and $L_y{=}2$ sensors in the two dimensions, respectively. The intersubarray displacements measured in half signal wavelength in the two dimensions are set to be $\Delta_2^x{=}L_x{+}3$ and $\Delta_2^y{=}L_y{+}3$, which are unknown for the frequency recovery. The SNR is calculated as $\mathrm{SNR}=1/\sigma_n^2$. The parameter λ is chosen to be $\lambda{=}\sigma_n(\sqrt{M/N}{+}1)$ as recommended in [12]. The results are averaged over $N_R{=}1000$ Monte-Carlo trials.

The root-mean-square error (RMSE) of the frequencies recovered by different methods is presented in Fig. 2. The estimation error of the proposed method (SI-SPARROW + MI-MD-ESPRIT) is compared to that of the conventional approach where MI-MD-ESPRIT is performed on the sample covariance matrix $\widehat{\boldsymbol{R}}$. Since the centro-symmetric arrays are used, we also perform the multidimensional Unitary ESPRIT (MD-Unitary-ESPRIT) [14, 15] on the sample covariance matrix $\widehat{\boldsymbol{R}}$. The MD-Unitary-ESPRIT method is similarly implemented by the simultaneous Schur decomposition. The stochastic Cramér-Rao Bound (CRB) in the partly calibrated case [9] is calculated as a reference for the performance evaluation. Similar to the conclusion in [3], Fig. 2 shows that, while the standard ESPRIT admits a significant degradation of the estimation quality for correlated sources, the incorporation of forward-backward averaging in the Unitary-ESPRIT typically leads to an enhanced error performance compared to the standard ESPRIT. On the other hand, the proposed method outperforms the MI-MD-ESPRIT and the MD-Unitary-ESPRIT in both asymptotic and non-asymptotic regions, especially in difficult scenarios, e.g., in the case with low SNR and/or with a limited number of snapshots. Nevertheless, the proposed method exhibits an asymptotic bias with the increase of the number of snapshots due to the $\ell_{2,1}$-regularization.

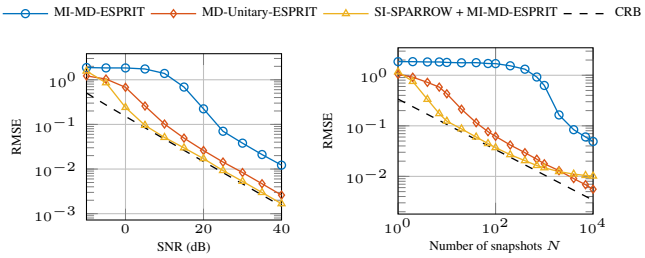

(a) RMSE vs. SNR for $N{=}5$ snapshots (b) RMSE vs. number of snapshots for SNR$=$0 dB

Fig. 2. Error performance for $N_S{=}2$ correlated sources.

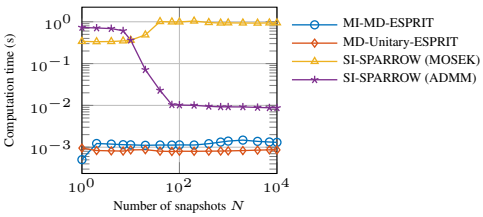

Fig. 3. Computation time vs. the number of snapshots for $N_S{=}2$ correlated sources and SNR$=$0 dB.

Next, the computational costs of the different methods, in particular, the two solution approaches for the SI-SPARROW problem in (11), are compared in Fig. 3. In the two solution approaches for the SI-SPARROW problem, suitable tolerances for the algorithm termination are selected so that they achieve similar precisions on the estimation quality. Both MI-MD-ESPRIT and MD-Unitary-ESPRIT admit closed-form solutions given the simultaneous diagonalization and, hence, they have the lowest computational costs. The two solution approaches for SI-SPARROW exhibit similar computational costs in the undersampled case, whereas, in the oversampled case, the ADMM algorithm possesses a significantly lower computational cost than the SDP implementation.

6. REFERENCES

[1] R. Schmidt, "Multiple emitter location and signal parameter estimation," *IEEE Trans. Antennas Propag.*, vol. 34, no. 3, pp. 276–280, 1986.

[2] R. Roy and T. Kailath, "ESPRIT-estimation of signal parameters via rotational invariance techniques," *IEEE Trans. Acoust. Speech Signal Process.*, vol. 37, no. 7, pp. 984–995, 1989.

[3] M. Haardt and J. A. Nossek, "Unitary ESPRIT: how to obtain increased estimation accuracy with a reduced computational burden," *IEEE Trans. Signal Process.*, vol. 43, no. 5, pp. 1232–1242, 1995.

[4] B. Friedlander, "A sensitivity analysis of the MUSIC algorithm," *IEEE Trans. Acoust. Speech Signal Process.*, vol. 38, no. 10, pp. 1740–1751, 1990.

[5] B. C. Ng and W. Ser, "Array shape calibration using sources in known locations," in *Proc. Singap. ICCS/ISITA '92*, 1992, pp. 836–840 vol.2.

[6] B. Liao and S. C. Chan, "A review on direction finding in partly calibrated arrays," in *Int. Conf. Digit. Signal Process.*, 2014, pp. 812–816.

[7] M. Pesavento, A. B. Gershman, and K. M. Wong, "Direction finding in partly calibrated sensor arrays composed of multiple subarrays," *IEEE Trans. Signal Process.*, vol. 50, no. 9, pp. 2103–2115, 2002.

[8] P. Parvazi, M. Pesavento, and A. B. Gershman, "Direction-of-arrival estimation and array calibration for partly-calibrated arrays," in *IEEE Int. Conf. Acoust. Speech Signal Process.*, 2011, pp. 2552–2555.

[9] C. M. S. See and A. B. Gershman, "Direction-of-arrival estimation in partly calibrated subarray-based sensor arrays," *IEEE Trans. Signal Process.*, vol. 52, no. 2, pp. 329–338, 2004.

[10] C. Steffens, P. Parvazi, and M. Pesavento, "Direction finding and array calibration based on sparse reconstruction in partly calibrated arrays," in *IEEE Sens. Array Multichannel Signal Process. Workshop*, 2014, pp. 21–24.

[11] C. Steffens, M. Pesavento, and M. E. Pfetsch, "A compact formulation for the $\ell_{2,1}$ mixed-norm minimization problem," *IEEE Trans. Signal Process.*, vol. 66, no. 6, pp. 1483–1497, 2018.

[12] C. Steffens, W. Suleiman, A. Sorg, and M. Pesavento, "Gridless compressed sensing under shift-invariant sampling," in *IEEE Int. Conf. Acoust. Speech Signal Process.*, 2017, pp. 4735–4739.

[13] J. Zhang and M. Haardt, "Channel estimation and training design for hybrid multi-carrier mmWave massive MIMO systems: The beamspace ESPRIT approach," in *25th Eur. Signal Process. Conf.*, 2017, pp. 385–389.

[14] M. D. Zoltowski, M. Haardt, and C. P. Mathews, "Closed-form 2-D angle estimation with rectangular arrays in element space or beamspace via unitary ESPRIT," *IEEE Trans. Signal Process.*, vol. 44, no. 2, pp. 316–328, Feb. 1996.

[15] M. Haardt and J. A. Nossek, "Simultaneous Schur decomposition of several nonsymmetric matrices to achieve automatic pairing in multidimensional harmonic retrieval problems," *IEEE Trans. Signal Process.*, vol. 46, no. 1, pp. 161–169, 1998.

[16] MOSEK ApS, "The MOSEK optimization toolbox for MATLAB. Version 10.0.22.," https://docs.mosek.com/10.0.22/toolbox/index.html.

[17] Y. Chi, L. L. Scharf, A. Pezeshki, and A. R. Calderbank, "Sensitivity to basis mismatch in compressed sensing," *IEEE Trans. Signal Process.*, vol. 59, no. 5, pp. 2182–2195, 2011.

[18] M. A. Herman and T. Strohmer, "General deviants: an analysis of perturbations in compressed sensing," *IEEE J. Sel. Top. Signal Process.*, vol. 4, no. 2, pp. 342–349, 2010.

[19] E. J. Candès and B. Recht, "Exact Matrix Completion via Convex Optimization," *Found Comput Math*, vol. 9, no. 6, pp. 717–772, 2009.

[20] S. Boyd, N. Parikh, E. Chu, B. Peleato, and J. Eckstein, "Distributed optimization and statistical learning via the alternating direction method of multipliers," *Found. Trends® Mach. Learn.*, vol. 3, no. 1, pp. 1–122, 2011.

[21] N. J. Higham, "Computing a nearest symmetric positive semidefinite matrix," *Linear Algebra and its Applications*, vol. 103, pp. 103–118, 1988.

[22] Y. Yang and M. Pesavento, "A unified successive pseudoconvex approximation framework," *IEEE Trans. Signal Process.*, vol. 65, no. 13, pp. 3313–3328, 2017.

[23] M. C. Grant and S. P. Boyd, "CVX: matlab software for disciplined convex programming, version 2.2," http://cvxr.com/cvx/, 2020.

[24] M. C. Grant and S. P. Boyd, "Graph implementations for nonsmooth convex programs," in *Recent Adv. Learn. Control*, Vincent D. Blondel, Stephen P. Boyd, and Hidenori Kimura, Eds., London, 2008, Lecture Notes in Control and Information Sciences, pp. 95–110, Springer.

[25] T. Fu and X. Gao, "Simultaneous diagonalization with similarity transformation for non-defective matrices," in *IEEE Int. Conf. Acoust. Speech Signal Process.*, 2006, vol. 4, pp. IV–IV.

[26] A. Barabell, "Improving the resolution performance of eigenstructure-based direction-finding algorithms," in *IEEE Int. Conf. Acoust. Speech Signal Process.*, 1983, vol. 8, pp. 336–339.